Anisotropic Rotation of Y_t-Base in n-Propanol at $-20\,^{\circ}C$ Studied by Frequency-Domain Fluorometry and Global Analysis

Ignacy Gryczynski, Stefan Paszyc, Wieslaw M. Wiczk, Gabor Laczko, Nanda Joshi, Henryk Szmacinski, and Henryk Cherek

University of Maryland at Baltimore, School of Medicine, Department of Biological Chemistry, 660 West Redwood Street, Baltimore, Maryland 21201, USA

Z. Naturforsch. **46a**, 269–274 (1991); received October 24, 1990

Dedicated to Professor Joseph R. Lakowicz on the occasion of his 40th birthday

The frequency response of the polarized emission of Y_t-base in n-propanol at $-20\,^{\circ}C$ was measured. Excitation wavelengths of 346, 312 and 285 nm were used for which the fundamental anisotropies were 0.32, 0.19 and 0.04, respectively. Additional data were obtained using CCl_4 to decrease the mean decay time from 10 ns to 0.7 ns. These nine sets of data were analyzed globally to recover the anisotropy decay law. Two correlation times, of about 146 ps and 502 ps, were needed for a good fit.

Introduction

Fluorescence polarization is very useful to detect reorientational motions of molecules, best quantified by the fluorescence anisotropy decay which depends upon the shape, size and optical properties of the rotating molecules as well as the dynamical properties of their surroundings [1–4]. Depending upon their spatial symmetry, molecules can have two or three different rotational diffusion coefficients, resulting in multiexponential anisotropy decays. To obtain adequate data, to recover closely spaced rotational correlation times is the most difficult task in applying this method, especially in the subnanosecond time range. In the present paper we report enhanced resolution as a result of a number of technical improvements. Firstly, anisotropy data were obtained in the frequency-domain which is known to provide good resolution of complex anisotropy decays [5–9]. Secondly, we performed "doubly" global measurements to provide extra information for the global analysis. The global data were obtained (a) using different excitation wavelengths, varying thereby the fundamental anisotropy from 0.04 to 0.32 (it is known that for different values of r_0 the various correlation times contribute differently to the anisotropy decay [10–12]) and (b) also varying the mean fluorescence decay time using CCl_4 as a collisional quencher (as the lifetime is decreased, the early time portion of the anisotropy decay contributes increasingly to the data [13, 14]). These nine data sets (3 wavelengths and 3 quencher concentrations) were analyzed by a global nonlinear least-squares algorithm.

Y_t-base (4,9-dihydro-4,6-dimethyl-9-oxo-1 H-1-imidazo-1,2 a purine) was examined because its structure is asymmetric (Scheme I) and the absorption and emission moments are probably not direct along the principle axes [15, 16]. Y_t-base is the simplest of the modified Y-like bases occurring in transfer ribonucleic acids specific to phenylalanine (t-RNA^{Phe}). It has been of special interest because of its strong fluorescence which offers a unique tool for probing the conformational properties of t-RNA^{Phe} [17, 18] or more simple synthetic compounds such as Y_t-$(CH_2)_n$-adenine [19–21].

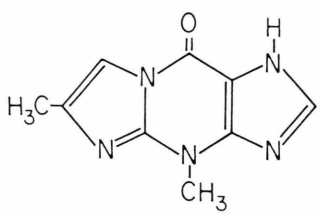

Scheme I. Chemical structure of Y_t-base.

Theory and Analysis

The present analysis is a modification of the global analysis technique suggested by Brand and coworkers [22, 23] and later, for multi-frequency data by this

Reprint requests to Prof. S. Paszyc, Department of Chemistry, Adam Mickiewicz University, 60-780 Poznan, Poland.

0932-0784 / 91 / 0300-0269 $ 01.30/0. – Please order a reprint rather than making your own copy.

laboratory [24, 25], which extends it to anisotropy decays with multiple excitation wavelengths and quencher concentrations.

The anisotropy decay at each excitation wavelength (λ) can be described by

$$r^{\lambda}(t) = \sum_i r_{0i}^{\lambda} \exp(-t/\Theta_i), \tag{1}$$

where λ indicates the excitation wavelength and Θ_i are the rotational correlation times. The values of r_{0i}^{λ} represent the amplitudes of the anisotropy which decay via the i-th correlation time when using an excitation wavelength λ. It should be noted that the correlation times are related, but not equal, to the rotational diffusion coefficients of the fluorophore about the principle axes [1–4]. In our analysis the individual r_{0i}^{λ} values were all variable parameters. If the data are adequate to recover the entire anisotropy decay then one expects $\sum r_{0i}^{\lambda}$ to be equal to r_0^{λ}, where r_0^{λ} is the anisotropy measured in the absence of rotational diffusion, that is under frozen or vitrified conditions. The value of r_{0i}^{λ} depends upon the average angle between the absorption and emission transition moments at each excitation wavelength. This dependence also affects the relative contribution of each rotational motion to the anisotropy decay [10–12].

In the frequency-domain the measured quantities are the phase angle difference between the parallel ($\parallel$) and perpendicular ($\perp$) components of the emission ($\Delta_{\omega}^{\lambda q} = \phi_{\perp} - \phi_{\parallel}$) and the ratio of the polarized modulated components of the emission ($\Lambda_{\omega}^{\lambda q} = m_{\parallel}/m_{\perp}$), each measured over a range of modulation frequencies (ω), excitation wavelengths (λ) and quencher concentrations (q).

In the non-linear least-squares analysis the calculated values (denoted by c) were obtained as

$$\Delta_{c\omega}^{\lambda q} = \arctan\left(\frac{D_{\parallel}^{\lambda q} N_{\perp}^{\lambda q} - N_{\parallel}^{\lambda q} D_{\perp}^{\lambda q}}{N_{\parallel}^{\lambda q} N_{\perp}^{\lambda q} + D_{\parallel}^{\lambda q} D_{\perp}^{\lambda q}}\right), \tag{2}$$

$$\Lambda_{c\omega}^{\lambda q} = \left(\frac{(N_{\parallel}^{\lambda q})^2 - (D_{\parallel}^{\lambda q})^2}{(N_{\perp}^{\lambda q})^2 + (D_{\perp}^{\lambda q})^2}\right)^{1/2}, \tag{3}$$

where

$$N_i^{\lambda q} = \int_0^{\infty} I_i^{\lambda q}(t) \sin \omega t \, dt, \tag{4}$$

$$D_i^{\lambda q} = \int_0^{\infty} I_i^{\lambda q}(t) \cos \omega t \, dt \tag{5}$$

and j represents the parallel or perpendicular component of the emission. These components of the emission are given by

$$I_{\parallel}^{\lambda q}(t) = \tfrac{1}{3} I_0^{\lambda q}(t) [1 + 2 r^{\lambda}(t)], \tag{6}$$

$$I_{\perp}^{\lambda q}(t) = \tfrac{1}{3} I_0^{\lambda q}(t) [1 - r^{\lambda}(t)], \tag{7}$$

where $I_0^{\lambda q}(t)$ is the decay of the total emission.

The goodness-of-fit of the anisotropy decay law (1) to the data is estimated from the value of the reduced chi-square:

$$\chi_R^2 = \frac{1}{\nu} \sum_{\omega,\lambda,q} \left(\frac{\Delta_{\omega}^{\lambda q} - \Delta_{c\omega}^{\lambda q}}{\delta \Delta}\right)^2 + \frac{1}{\nu} \sum_{\omega,\lambda,q} \left(\frac{\Lambda_{\omega}^{\lambda q} - \Lambda_{c\omega}^{\lambda q}}{\delta \Lambda}\right)^2, \tag{8}$$

where ν is the number of degrees of freedom (number of data points minus the number of floating parameters), and $\delta\Delta$ and $\delta\Lambda$ are the uncertainties in the measured values. In the presently reported work the data at all ω, λ and q are analyzed simultaneously to recover a single set of correlation times and three sets of amplitudes (r_{0i}), one set for each excitation wavelength.

The modulation data are presented as the modulated anisotropy

$$r_{\omega}^{\lambda q} = (\Lambda_{\omega}^{\lambda q} - 1)/(\Lambda_{\omega}^{\lambda q} + 2). \tag{9}$$

The values of $r_{\omega}^{\lambda q}$ can be compared with those of the steady-state anisotropy ($r^{\lambda q}$) and the fundamental anisotropy r_0^{λ}. At low modulation frequencies $r_{\omega}^{\lambda q}$ is nearly equal to $r^{\lambda q}$. At high modulation frequencies $r_{\omega}^{\lambda q}$ approaches r_0^{λ} [9].

It should be noted that the intensity decays of Y_t-base become increasingly heterogeneous in the presence of quencher. This transient effect is due to the translational diffusion of the quencher [27–29]. The rotation-free intensity decays ("magic angle" observation polarizer) were measured at each excitation wavelength and quencher concentration.

The multi-exponential model [24, 29],

$$I_0^{\lambda q}(t) = \sum_i \alpha_i^{\lambda q} \exp(-t/\tau_i^{\lambda q}) \tag{10}$$

was fitted to the data.

The parameters from the double exponential fit were used in (6) and (7). These parameters ($\alpha_i^{\lambda q}$ and $\tau_i^{\lambda q}$) were, as expected, strongly dependent on the quencher concentration. Equivalent values were obtained for each excitation wavelength for the same concentration of quencher. The fluorescence intensity decay of Y_t-base in n-propanol at -20 °C does not depend on the excitation wavelength. The parameters α_i^q and τ_i^q were obtained from simultaneous analyses (three excitation wavelengths) for each quencher concentration.

Materials and Methods

Frequency-domain measurements were performed using the 2 GHz phase-and-modulation fluorometer described previously [30]. This instrument was modified by addition of a second pyridine 2 dye laser. After frequency doubling, this dye laser provided excitation at 346 nm. The frequency-doubled output of a rhodamine 6G laser was used for excitation at 312 and 285 nm.

All solutions were miscible with n-propanol at -20 °C. Y_t-base was purified by HPLC. The laser beam was expanded to about 5 mm in diameter to decrease its local intensity. The emission was observed through a Corning 3-74 filter. We did not notice any significant loss intensity or change in phase or modulation values during the experiment, suggesting that photodecomposition was not significant.

Results and Discussion

The excitation anisotropy spectrum in vitrified solution (propylene glycol, -60 °C) is shown in Figure 1. Three excitation wavelengths (285, 312 and 346 nm) were chosen. As indicated by the arrows, these wavelengths yield r_0 values of 0.04, 0.19 and 0.32, respectively. In Fig. 1, the absorption and emission spectra of Y_t-base are also shown. The emission was quenched by CCl_4, resulting in quenching of the emission by about 75% and 85% at CCl_4 concentrations of 0.5 and 1 M, respectively. The frequency-domain intensity data are shown in Fig. 2, in the absence (●) and presence (○) of 1 M CCl_4. In the absence of CCl_4 the intensity decay is biexponential ($\chi_R^2 = 1.3$) but very close to being monoexponential ($\chi_R^2 = 9.6$). In the presence of quenching the decay becomes strongly heterogeneous and can not reasonably approximated by the monoexponential model ($\chi_R^2 = 864$) compared with 3.2 for the best biexponential fit. Each intensity decay was parametrized using a biexponential model. The results of these analyses are summarized in Table 1.

As can be judged by the increases in χ_R^2 for the single decay time fits, quenching makes the intensity decays increasingly heterogeneous. It should be noted that the intensity decays are not dependent upon the excitation wavelength. At each quencher concentration, the same intensity decay parameters ($\alpha_i^{\lambda,q}$ and $\tau_i^{\lambda,q}$) were obtained for each of the different excitation wavelengths.

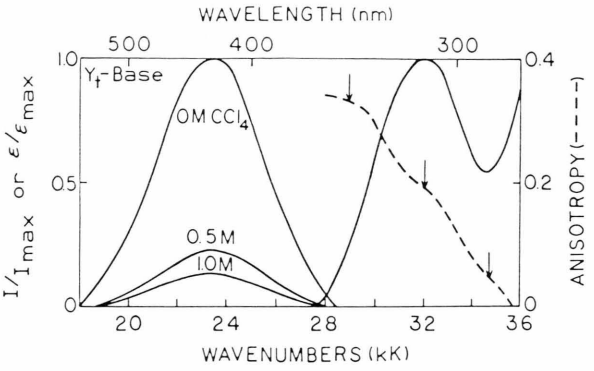

Fig. 1. Absorption, emission and anisotropy (- - - -) spectra of Y_t-base. The anisotropy values (r_0) were measured in propylene glycol at -60 °C.

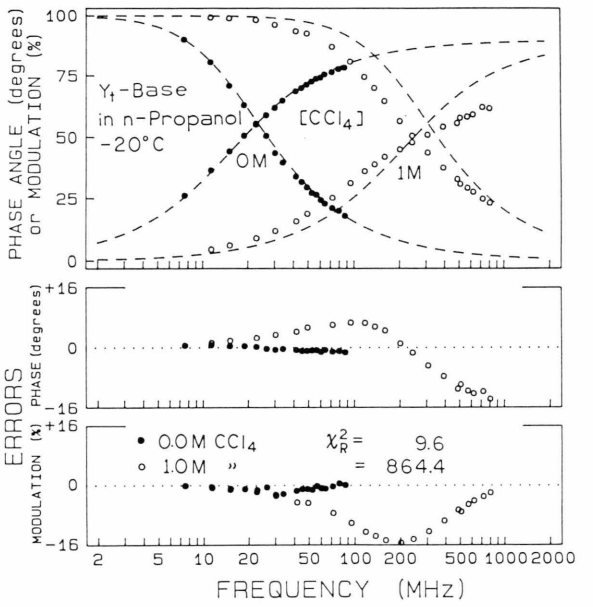

Fig. 2. Frequency-response of the emission of Y_t-base with (○) and without (●) 1 M CCl_4. The dashed lines show the best fit to the data for a monoexponential decay, the deviations from "perfect" fits being displayed in the lower half of the figure.

The frequency-domain anisotropy data are shown in Figure 3. The values are seen to depend upon both the excitation wavelength and the quencher concentration. At high modulation frequencies the $r_\omega^{\lambda,q}$ values tend toward the r_0^λ value for the appropriate excitation wavelength. The phase angles decrease with increasing concentration of CCl_4.

The data in Fig. 3 were analyzed globally to recover one and two correlation times (Table 2). In the latter case, the portion of the total anisotropy associated

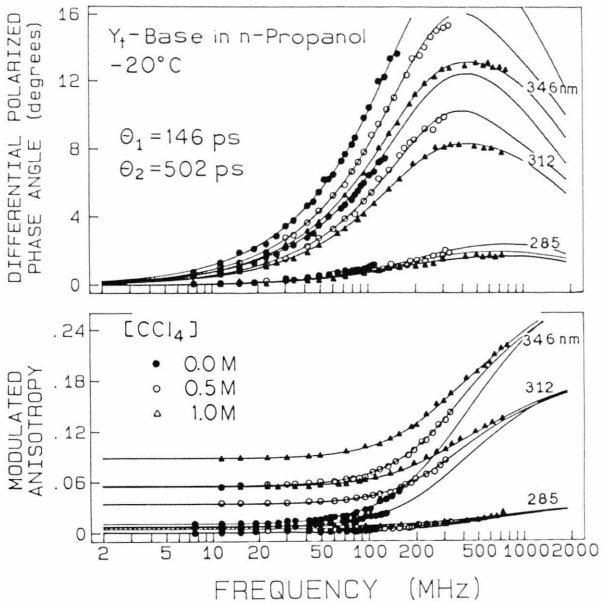

Fig. 3. Frequency-domain anisotropy data for Y_t-base. In the upper panel, at each excitation wavelength, the decreasing phase angles are for 0, 0.5 and 1 M CCl_4. In the lower panel, at each excitation wavelength the increasing modulated anisotropies are for 0, 0.5 and 1 M CCl_4.

Table 1. Intensity decays of Y_t-base in n-propanol at -20 °C.

$[CCl_4]$	Model[a]	α_i	f_i^q (ns)[b]	τ_i^q (ns)	τ^q (ns)[c]	χ_R^2
0	1 τ	1	1	10.08		9.6
	2 τ	0.070	0.018	2.56		
		0.930	0.982	10.55	10.41	1.3
0.5	1 τ	1	1	1.64		288.9
	2 τ	0.379	0.062	0.21		
		0.621	0.938	1.98	1.86	2.4
1.0	1 τ	1	1	0.76		864.4
	2 τ	0.598	0.188	0.20		
		0.402	0.812	1.31	1.10	3.2

[a] 1 τ denotes single exponential model, etc.
[b] The fractional intensities (f_i^q) are given by $f_i^q = \alpha_i^q \tau_i^q / \sum \alpha_i^q \tau_i^q$.
[c] The mean decay times were calculated using $\tau^q = \sum f_i \tau_i^q$.

Table 2. Global analysis of the anisotropy decay of Y_t-base in n-propanol at -20 °C.

Model[a]	Θ_i (ps)	r_{0i}^λ at			χ_R^2
		346 nm	312 nm	285 nm	
1 Θ	390	0.275	0.170	0.026	5.8
2 Θ	146 ± 5[b]	0.109	0.063	0.021	
	502 ± 4[b]	0.195	0.122	0.012	2.1
	r_{0i}^λ (for 2 Θ):	0.304	0.185	0.033	
	Measured r_0:	0.32	0.19	0.03	

[a] 1 Θ denotes the fit to one correlation time, etc.
[b] Uncertainties in Θ_i from the diagonal elements of the covariance matrix [31].

with each of the two correlation times was a variable parameter. The two-correlation-time analysis yields eight parameters: six r_{0i} and two Θ_i values. The single correlation time model could not be adequately fit to the data, as is seen from $\chi_R^2 = 5.8$ (Table 2). Using a two correlation time model, χ_R^2 was three times smaller and correlation times of 146 ps and 502 ps were recovered. Our confidence in the analysis is enhanced by the recovery of the expected values for the total anisotropy ($\sum r_{0i}^\lambda$). At each excitation wavelength $\sum r_{0i}^\lambda$ was very close to r_0^λ measured in frozen solution. The recovered rotational correlation times are closely spaced, spanning only a 3-fold range. In propylene glycol at -5 °C, on the other hand, the span was 6-fold (2.1 ns and 12.1 ns) [25].

Finally, we questioned the uncertainties in the correlation times. An estimation of the uncertainty is provided by the least-squares analysis, in particular by the diagonal elements of the covariance matrix [31]. This estimation is correct only if there is no correlation between the fitted parameters, i.e. provided they are not themselves functions of common independent parameters. This is, of course, not the case here since the correlation times are actually functions of common rotational diffusion coefficients. However, the thus estimated uncertainties are near 5 ps (Table 2), thus the two correlation times, with their associated uncertainties, do not overlap. We also performed a more rigorous analysis of the uncertainties. We examined the χ_R^2 surfaces for the parameters. These surfaces are constructed by holding, in turn, each parameter fixed at a given value, followed by reminimalization of χ_R^2 by variation of the other parameters. The procedure accounts for all possible correlations between the parameters and reveals the range of values consistent with the data. For the correlation times, the result of this procedure is shown in Figure 4. The dashed line indicates the value of χ_R^2 expected in 33% of the time due to random errors. Because of the lack of rigorous theory for uncertainties, we used this elevation in χ_R^2 to define the uncertainty of the correlation times. Based on this approach, the Θ_i values were found to have uncertainties of about 20%. We believe that this method overestimates the uncertainties in the correlation times by about two-fold. It should also be noted that distinguishable correlation times for Y_t-base in n-propanol as the three-correlation-time analysis yielded two correlation times identical at 502 ps.

Since the anisotropy decay is determined by the size and shape of the fluorophore, we expect this decay to

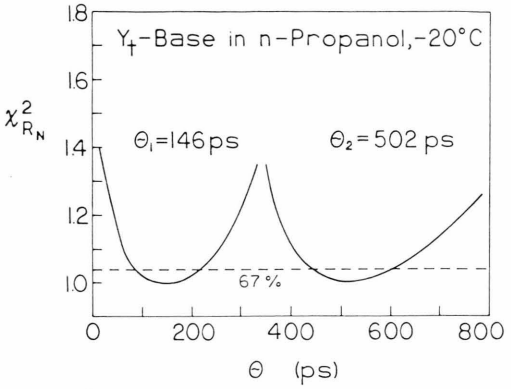

Fig. 4. χ^2_R surface for the two correlation times of Y_t-base.

reflect the interactions of Y_t-base with its solvent shell. The Y_t-base molecule is strongly asymmetric, and it is difficult to determine its shape. We approximated the Y_t-base as an oblate spheroid with diameters of 9.5 and 4 Å in the equatorial and polar axes. The value of 4 Å corresponds to the thickness of the molecule. The longer axes estimate of 9.5 Å did not include the methyl group in position 6. It should be noted that increasing the overall molecule dimensions increases the calculated correlation times without affecting their relative values. The volume of this spheroid is 190 Å^3. The rotational diffusion coefficients of an oblate rotor may be obtained from the solution of the Navier-Stokes equation subject to certain boundary conditions. With stick boundary conditions (Stokes-Einstein theory):

$$\Theta_i = \frac{1}{6D_i} = \eta \lambda_i \frac{V}{kT} = \eta C_i , \tag{11}$$

where V is the volume of the molecule, η the viscosity, and D_i and C_i are the diffusion and friction coefficients, respectively. The λ_i depend only on the shape of the molecule, and the values are tabulated [32, 33]. Sticking may occur in systems where strong interactions are present between the fluorophore and solvent molecules. The calculated stick boundary correlation times for the oblate spheroid model used here are $\Theta_1 = 1/6D_\perp = 451$ ps, $\Theta_2 = 1/(5D_\perp + D_\parallel) = 466$ ps and $\Theta_3 = 1/(2D_\perp + D_\parallel) = 520$ ps according Tao [32]. These results are in good agreement with the longer measured correlation time 502 ps. The shorter correlation time observed (146 ps) cannot be explained using stick boundary hydrodynamics. In systems where the solvent and solute molecules are both of molecular dimensions and no strong interactions occur, it is more appropriate to employ slip boundary conditions (i.e. no tangential stress). Here the resistance to the motion arises from the fact that, for non-spherical molecules, some solvent molecules must be displaced as the fluorophore rotates. The coefficient of friction with slip for a spheroid rotating about its symmetry axis is zero. For slip boundary conditions, Pecora and coworkers [34, 35] proposed

$$\Theta_i = \frac{1}{6D_i} = \eta C_i' + \Theta_i^0 \tag{12}$$

with

$$C_i' = \lambda_i' \frac{V}{kT} . \tag{13}$$

The λ_i' have been computed numerically by Hu and Zwanzig [36]. The value of Θ_i^0, corresponding to the inertial moment, is generally out of reach of fluorescence anisotropy data. For the oblate spheroid discussed, the ratio of slip to stick friction coefficients is 0.37 [33, 36], leading to calculated slip boundary correlation times $\Theta_1 = 168$ ps, $\Theta_2 = 173$ ps and $\Theta_3 = 192$ ps, which are in reasonable agreement with the shorter correlation time of 146 ps.

Acknowledgement

This work was supported by grants DMB-8502835 and DMB-8511065 from the National Science Foundation, and grant GM 39617 from the National Institutes of Health and partly within the Ministry of National Education project RP.II.13.2.15.

[1] G. G. Belford, R. L. Belford, and G. Weber, Proc. Natl. Acad. Sci. US **69,** 1392 (1972).
[2] E. W. Small and I. Isenberg, Biopolymers **16,** 1907 (1977).
[3] T. J. Chuang and K. B. Eisenthal, J. Chem. Phys. **57,** 5094 (1972).
[4] M. D. Barkley, A. Kowalczyk, and L. Brand, J. Chem. Phys. **75,** 3581 (1981).
[5] E. Gratton and M. Limkeman, Biophys. J. **44,** 315 (1983).
[6] J. R. Lakowicz and B. P. Maliwal, Biophys. Chem. **21,** 61 (1985).
[7] H. P. Haar, U. K. A. Klein, F. W. Hafner, and M. Hauser, Chem. Phys. Lett. **49,** 563 (1977).
[8] J. R. Lakowicz, I. Gryczynski, and H. Cherek, J. Biol. Chem. **261,** 2240 (1986).
[9] B. P. Maliwal and J. R. Lakowicz, Biochim. Biophys. Acta **873,** 161 (1986).
[10] G. Weber, J. Chem. Phys. **55,** 2399 (1971).
[11] G. Weber, J. Chem. Phys. **66,** 4081 (1977).

[12] L. Brand, J. R. Knutson, L. Davenport, J. M. Beechem, R. E. Dale, D. G. Walbridge, and A. Kowalczyk, in: Spectroscopy and the Dynamics of Molecular Biological Systems (P. M. Bayley and R. E. Dale, eds.), Academic Press, New York 1985, pp. 259–305.
[13] J. R. Lakowicz, H. Cherek, I. Gryczynski, N. Joshi, and M. L. Johnson, Biophys. J. **51,** 755 (1987).
[14] J. R. Lakowicz, H. Szmacinski, and I. Gryczynski, Photochem. Photobiol. **47,** 31 (1988).
[15] I. Gryczynski, Ch. Jung, A. Kawski, S. Paszyc, and B. Skalski, Z. Naturforsch. **34a,** 172 (1979).
[16] I. Gryczynski, Z. Gryczynski, A. Kawski, and S. Paszyc, Photochem. Photobiol. **39,** 319 (1984).
[17] W. E. Blumberg, R. E. Dale, J. Eisinger, and D. M. Zuckerman, Biopolymers **13,** 1607 (1974).
[18] B. D. Wells and J. R. Lakowicz, Biophys. Chem. **26,** 39 (1987).
[19] I. Gryczynski, A. Kawski, S. Paszyc, and B. Skalski, J. Photochem. **20,** 71 (1982).
[20] I. Gryczynski, A. Kawski, S. Paszyc, and B. Skalski, Z. Naturforsch. **35a,** 1265 (1980).
[21] I. Gryczynski, A. Kawski, S. Paszyc, B. Skalski, and A. Tempczyk, J. Photochem. **30,** 153 (1985).
[22] J. M. Beechem, J. R. Knutson, J. B. A. Ross, B. W. Turner, and L. Brand, Biochemistry **22,** 6054 (1983).
[23] J. R. Knutson, J. M. Beechem, and L. Brand, Chem. Phys. Lett. **102,** 501 (1983).
[24] J. R. Lakowicz, G. Laczko, H. Cherek, E. Gratton, and M. Limkeman, Biophys. J. **46,** 463 (1984).
[25] I. Gryczynski, H. Cherek, G. Laczko, and J. R. Lakowicz, Chem. Phys. Lett. **135,** 193 (1987).
[26] J. R. Lakowicz, M. L. Johnson, I. Gryczynski, N. Joshi, and G. Laczko, J. Phys. Chem. **91,** 3277 (1987).
[27] N. Joshi, M. L. Johnson, and J. R. Lakowicz, Chem. Phys. Lett. **135,** 200 (1987).
[28] I. Gryczynski, M. L. Johnson, and J. R. Lakowicz, Biophys. Chem., submitted for publication.
[29] E. Gratton, J. R. Lakowicz, B. P. Maliwal, H. Cherek, G. Laczko, and M. Limkeman, Biophys. J. **46,** 479 (1984).
[30] J. R. Lakowicz, G. Laczko, and I. Gryczynski, Rev. Sci. Instrum. **57,** 2499 (1986).
[31] P. R. Bevington, Data Reduction and Error Analysis for the Physical Sciences, McGraw-Hill, New York 1969, pp. 242, 313–322.
[32] T. Tao, Biopolymers **8,** 609 (1967).
[33] G. R. Fleming, Chemical Applications of Ultrafast Spectroscopy, Oxford University Press, New York 1986, Chapter 6.
[34] G. R. Alms, D. R. Bauer, J. I. Brauman, and R. Pecora, J. Chem. Phys. **59,** 5321 (1973).
[35] D. R. Bauer, G. R. Alms, J. I. Brauman, and R. Pecora, J. Chem. Phys. **61,** 2255 (1975).
[36] C. M. Hu and R. Zwanzig, J. Chem. Phys. **60,** 4354 (1974).
[37] G. R. Fleming, A. E. W. Knight, J. M. Morris, R. J. Robins, and G. W. Robinson, Chem. Phys. Lett. **51,** 399 (1977).